Materials Transactions, Vol. 43, No. 9 (2002) pp. 2205 to 2212

Comparison of the Characteristics of Nanocrystalline Ferrite in Fe–0.89C Steels with Pearlite and Spheroidite Structure Produced by Ball Milling

Yan Xu[1,*], Minoru Umemoto[2] and Koichi Tsuchiya[2]

[1]*Institute of Metal Research, The Chinese Academy of Sciences, Shenyang 110015, P.R. China*
[2]*Department of Production Systems Engineering, Toyohashi University of Technology, Toyohashi 441-8580, Japan*

Nanocrystalline ferrite formation by ball milling in Fe–0.89C steels with initial pearlite and spheroidite microstructures and their annealing behaviors have been studied through microstructural observation and microhardness measurement. It was found that nanocrystalline ferrite first forms near the surface of powders due to localized severe deformation. The microhardness of nanocrystalline ferrite regions is much higher than that of work-hardening regions. The dissolution of cementite was observed together with the nanocrystallization of ferrite. The nanocrystallization rate of pearlite powder is faster than that of spheroidite powder due to higher work-hardening rate and smaller cementite size. After long time ball milling, the equiaxed nanocrystalline ferrite with less than 10 nm grain size forms in the whole powders of both pearlite and spheroidite structures, and the cementite dissolves completely. By annealing the milled pearlite and spheroidite powders, recrystallization was observed in the work-hardening regions, while continuous grain growth was observed in the nanocrystalline ferrite region. After annealing, microhardness of the former nanocrystalline ferrite region is always higher than that of the former work-hardening region when compared at the same annealing condition. The grain growth rate of nanocrystalline ferrite produced from pearlite structure is lower than that of spheroidite structure due to the finer grains.

(Received March 20, 2002; Accepted July 2, 2002)

Keywords: *ball milling, pearlite, spheroidite, nanocrystalline ferrite, deformation, cementite dissolution, annealing, grain growth*

1. Introduction

Mechanical properties of engineering materials can be improved by refining their microstructures. Various severe plastic deformation processes, such as cold rolling,[1,2] equal channel angular pressing,[3,4] torsion straining under high pressure,[5,6] and ball milling,[7–9] were developed to synthesize ultra-fine grained materials. Among these, ball milling is the most effective method to refine the grains down to 10 nm for most of metals, alloys and intermetallics.[7–13]

To improve mechanical properties, microstructure refinement has been studied extensively in steels. Recently, the formation of nanocrystalline ferrite in Fe–C alloys (including pure iron) by ball milling has been reported.[7,8,14–19] Various mechanisms of nanocrystallization have been proposed by many researchers according to their experimental results. It has been generally understood that ball milling gradually refine the grain size to the final nanocrystalline structure. However, our previous works[14,17–19] revealed that nanocrystallization in steels by ball milling is not a gradual process, but there is a sharp transition from work-hardening state to nanocrystalline state.

Pearlite steel with fine lamellar structure has high strength and excellent drawability. High strength wires used for tire cord, springs, wire rope and suspension cable were produced by heavy drawing. The presence of nanoscale fibrous ferrite in the pearlite steel wire is thought to contribute to the high strength.[20] Cementite dissolution during wire drawing is an attractive topic and studied by many researchers.[20–24] The nanocrystallization of pearlite and spheroidite steels has been investigated by ball milling.[25,26] The comparison of nanocrystallization in steels with pearlite and spheroidite microstructure by ball milling will give a useful information to understand the influence of microstructure factors on nanocrystallization.

The thermal stability of nanocrystal is another important issue and has been studied by several researchers.[8,14,19,27–29] It was found that grain growth rate of nanocrystalline ferrite is much lower than that of conventional coarse grained ferrite. Lower atom jump frequency or higher activation energy for diffusion in nanocrystalline ferrite was considered to be responsible to this phenomenon. The pinning effect which retards the grain boundary migration was also proposed to explain the slow grain growth rate of nanocrystalline materials.[29,30] However the mechanism of slow grain growth in nanocrystalline materials is still unclear.

In the present study, the formation process of nanocrystalline ferrite by ball milling in Fe–0.89C steels with pearlite and spheroidite microstructures was compared in detail. The thermal stability of nanocrystalline ferrite was studied by annealing the ball-milled powders. Special attention was paid to find the influence of microstructure on the nanocrystallization process.

2. Experimental Procedures

The material used in the present study was a steel (0.887C, 0.25Si, 0.50Mn, 0.005P, 0.0044S, 0.036Al, 0.0048N, 0.003Ni, 0.30Cr and 0.003Ti at mass%) with pearlite microstructure. To obtain spheroidite structure, specimens were first austenitized at 1173 K for 3.6 ks followed by oil quenching to obtain martensite. Spheroidising treatment was subsequently carried out at 983 K for 79.2 ks. The chips with a thickness of less than 1 mm and a length of several mm

*Doing this research work in the Department of Production Systems Engineering, Toyohashi University of Technology, Toyohashi 441-8580, Japan.

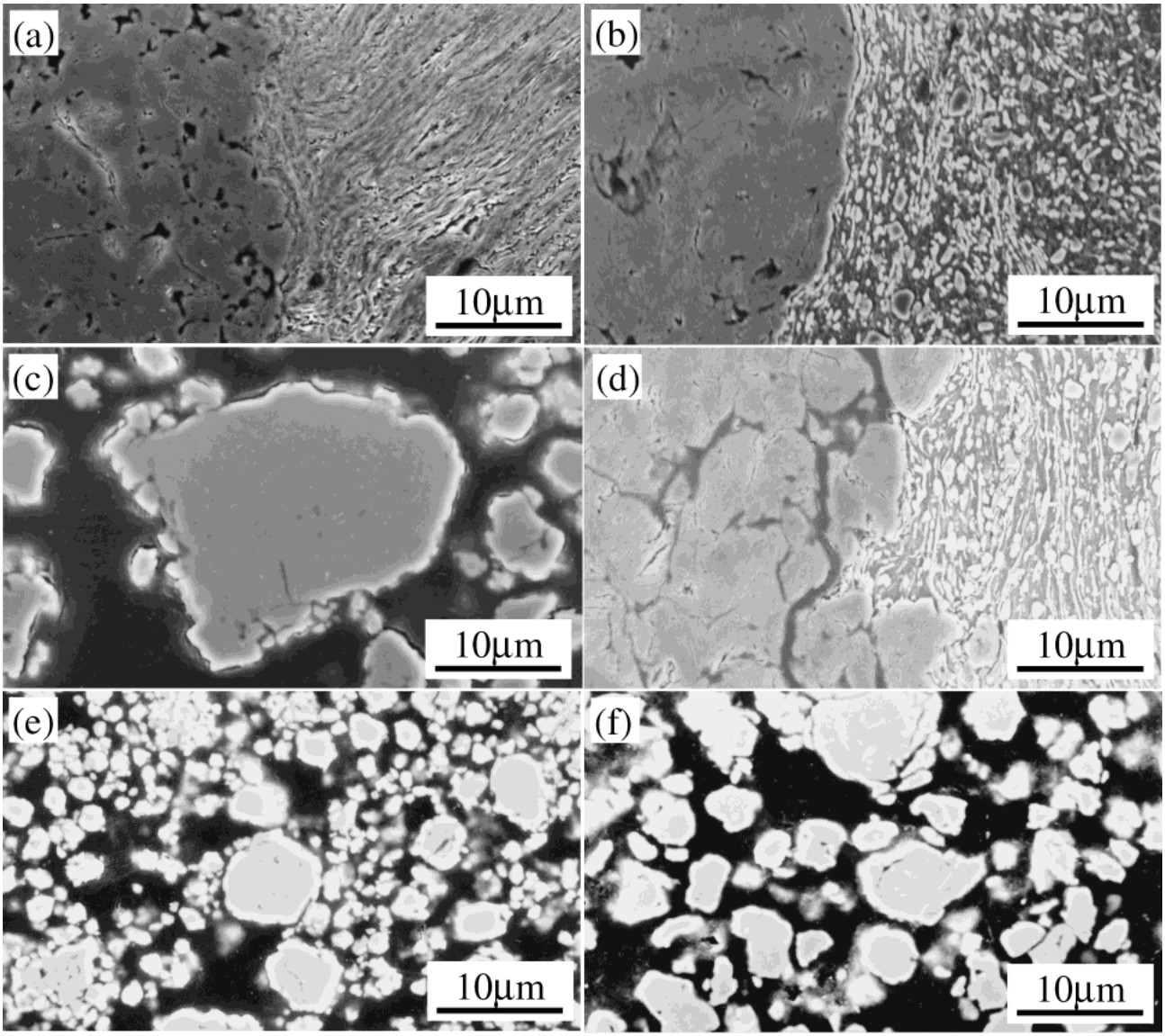

Fig. 1 Microstructure evolution of ((a), (c), (e)) pearlite and ((b), (d), (f)) spheroidite powders with ball milling for (a), (b) 360 ks; (c), (d) 720 ks and (e), (f) 1800 ks.

were cut from the specimens with pearlite and spheroidite microstructure, respectively. These chips were loaded into a stainless vial with steel balls (SUJ2) and ball milled under a pure Ar atmosphere using a conventional horizontal ball mill. The weight ratio of ball to powder was 100 : 1 and the milling time was up to 1800 ks. Part of the milled powders were sealed in quartz tubes with pure Ar protective atmosphere and annealed at different temperature for 3.6 ks. The as-milled and annealed powders were subjected to structural observations by scanning electron microscope (SEM, JEOL JSM-6300) and scanning probe microscope (SPM, SHIMADZU SPM-9500 J2) after etching with 3% Nital. Transmission electron microscopic (TEM) observations were carried out on a Hitachi H-800 microscope working at 200 KV. High-resolution electron microscopic (HREM) observations were performed on JEOL JEM-2010 working at 200 KV. Microhardness measurement was carried out using a MVK-G1 Vickers hardness tester.

3. Results

3.1 Microstructure and microhardness evolution along ball milling time

3.1.1 Microstructure evolution

Figure 1 shows the microstructural evolution of pearlite and spheroidite powders with milling time. After ball milled for 360 ks, two types of microstructures appeared in both pearlite and spheroidite powders (Figs. 1(a), (b)). One is a uniform structure observed near the surface of powders (the left hand side of each picture), which does not show any distinguishable details after etching with Nital. Cementite is hard to be observed in this region by SEM. This structure was found to be nanocrystalline ferrite by TEM observation as would be mentioned below. Another is a work-hardening structure in the interior of the powders (the right hand side of each picture), *i.e.* deformed pearlite structure (Fig. 1(a)) and deformed ferrite grains with spherical cementite (Fig. 1(b)). With increasing milling time to 720 ks, the size of pearlite powder becomes finer (less than 20 μm). The microstructures of all the

powders become uniform structure (nanocrystalline ferrite) irrespective of their size (Fig. 1(c)). The size of spheroidite powder after ball milling for 720 ks is larger than that of pearlite powder. Two types of microstructures still remain in most of the large spheroidite powder (Fig. 1(d)), and uniform structure (nanocrystalline ferrite) is seen in the smaller powder. Longer milling time to 1800 ks leads to the further refinement of powder and formation of a uniform structure (nanocrystalline ferrite) in all spheroidite powders (Figs. 1(e), (f)). The average size of powder is finer in pearite than spheroidite. It is clear that the formation rate of nanocrystalline ferrite by ball milling is faster in pearlite (completed by 720 ks milling) than that in spheroidite powder (completed by 1800 ks milling). This indicates that the size of starting microstructure has various influences on the nanocrystallization process.

The detailed observation of microstructure evolution was done by TEM. Figure 2 is typical TEM micrographs of the work-hardened region in the interior of pearlite powders milled for 360 ks. High density of dislocations was observed in the ferrite lamellae, and the cementite particles were observed in the prior cementite lamellae (Fig. 2(a)). In other region, equiaxed ferrite grains with cementite particles are seen due to further plastic deformation (Fig. 2(b)). Figure 3 shows the TEM image of work-hardening region in the interior of spheroidite powder milled for 360 ks. High density of dislocations was also observed in the deformed ferrite grains.

Figure 4 shows the TEM image of the area near the surface of pearlite powder milled for 360 ks. Equiaxed nanocrystalline ferrite with an average grain size less than 20 nm was observed. The bright field image and the selected area diffraction patterns (SAD) of this region show that cementite has dissolved into ferrite. It is considered that cementite particles receive severe deformation, fracture into small particles and dissolve into nanocrystalline ferrite grains. Figure 5 shows the TEM images of the area near the surface of spheroidite powder milled for 360 ks. Two types of microstructures were observed. One is layered nanocrystalline ferrite structure with 10–50 nm thickness as is shown in Fig. 5(a). The bright field image and SAD of this region show that a small fraction of cementite still remains as fine particles. The HREM image (Fig. 5(b)) of the layered nanocrystalline ferrite indicates that the grain boundary of layered nano-structure is not of dislocation cell wall type but of granular type like conventional high angle grain boundary. The misorientation angle between the adjacent layers was generally high. For instance, the misorientation angles in Fig. 5(b) measured from (110) plane is 18°. The other type of microstructure is an equiaxed nanocrystalline ferrite with grain size less than 20 nm (Fig. 5(c)). It

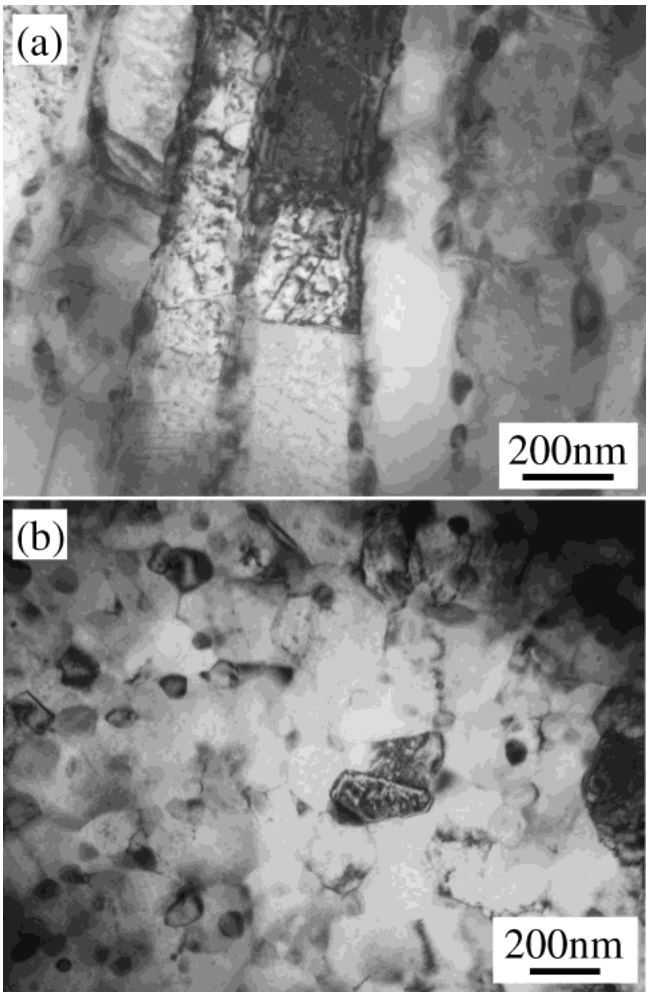

Fig. 2 Typical TEM images of the work-hardening region in the pearlite powders milled for 360 ks.

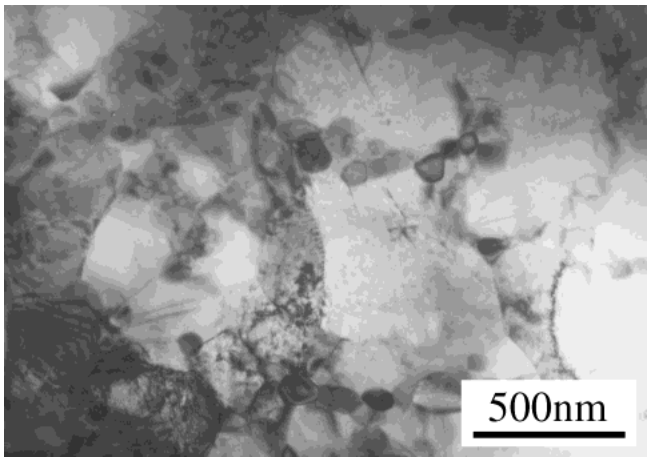

Fig. 3 Typical TEM image of the work-hardening region of spheroidite powders milled for 360 ks.

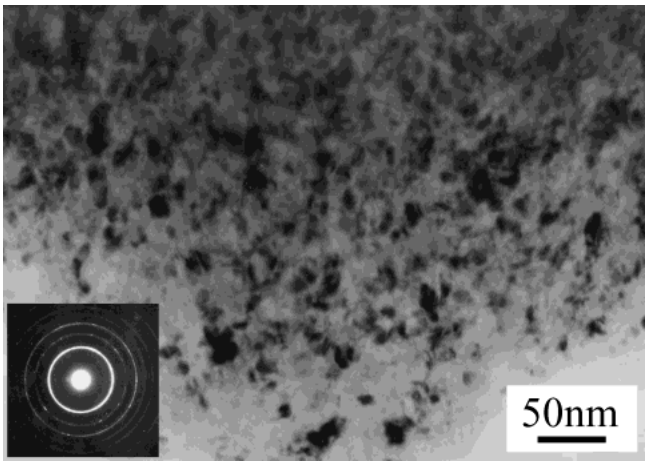

Fig. 4 Typical TEM image of the nanocrystalline ferrite in the pearlite powders milled for 360 ks.

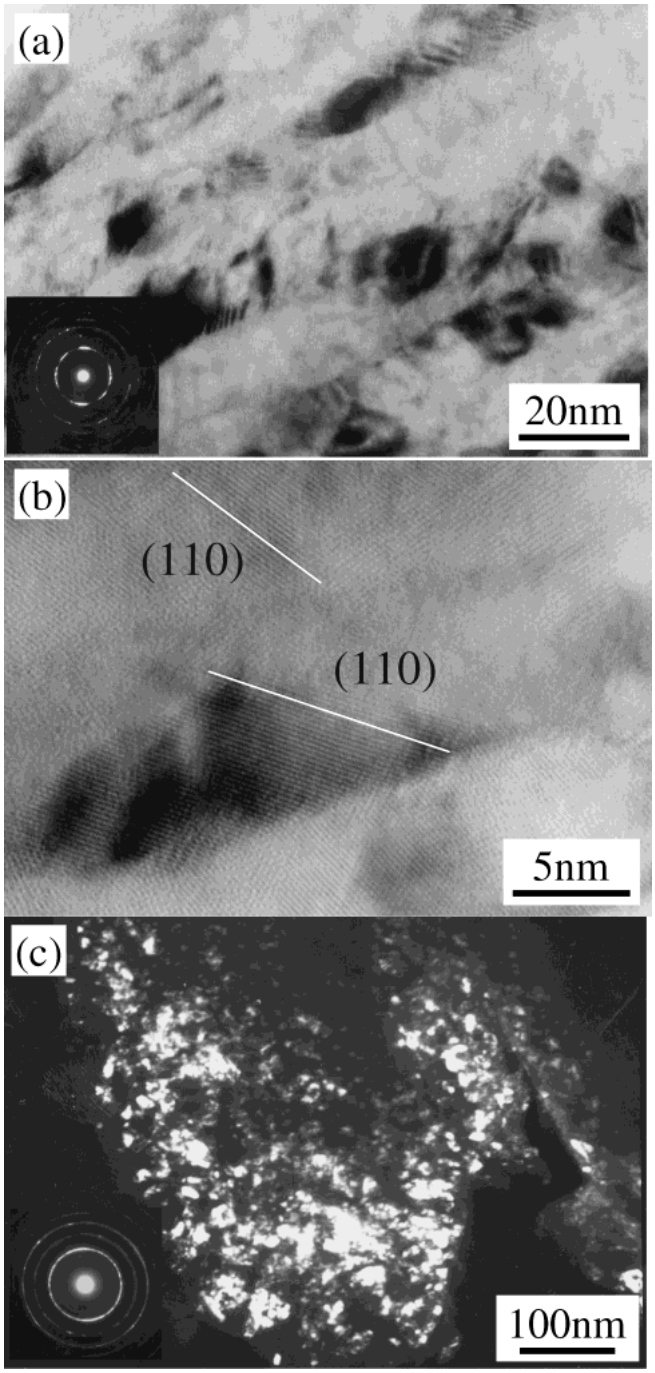

Fig. 5 Typical TEM images of the nanocrystalline ferrite in the spheroidite powders milled for 360 ks: (a) layered nanocrystalline ferrite, (b) high resolution image of layered nanocrystalline ferrite, (c) equiaxed nanocrystalline ferrite.

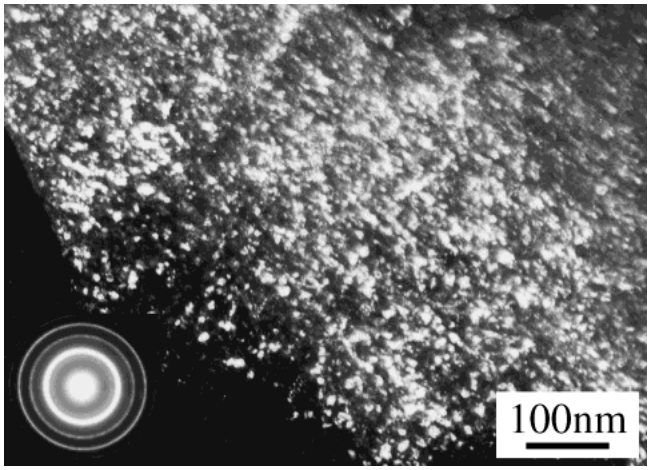

Fig. 6 Typical TEM image of the nanocrystalline ferrite in the pearlite powders milled for 1800 ks.

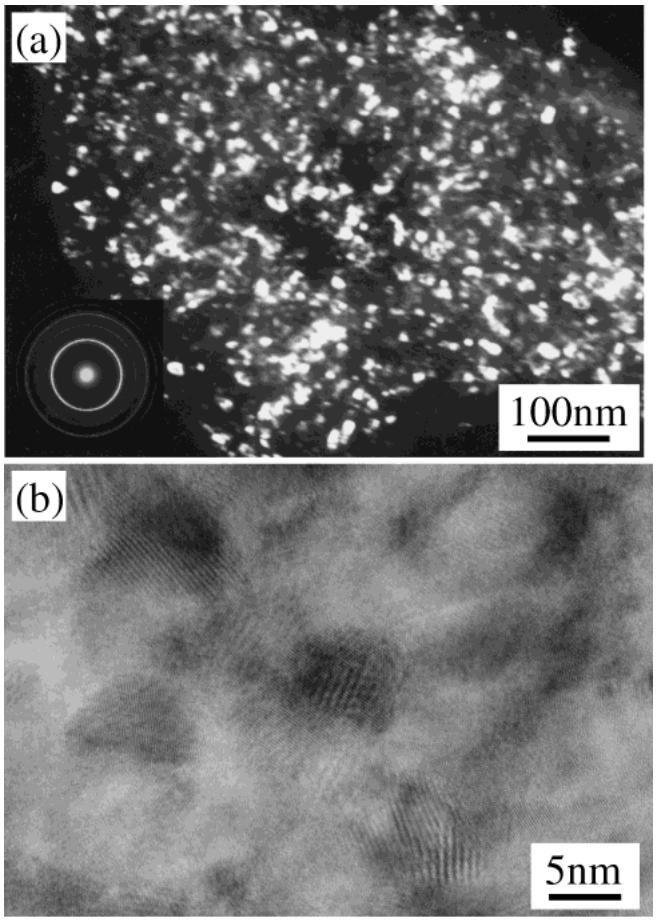

Fig. 7 Typical TEM images of the equiaxed nanocrystalline ferrite in the spheroidite powders milled for 1800 ks: (a) lower magnification and (b) high resolution images.

is considered that layered nanocrystalline ferrite will evolve into equiaxed nanocrystalline ferrite with further deformation. The volume fraction of layered nanocrystalline ferrite is much larger than that of equiaxed nanocrystalline ferrite in this milling condition (360 ks).

Figure 6 shows the TEM image of pearlite powders milled for 1800 ks. The microstructure of the whole powders is the uniform equiaxed nanocrystalline ferrite with grain size less than 10 nm. The bright field image and SAD indicate that the cementite particles have completely dissolved. Figure 7 shows the TEM images of spheroidite powders milled for 1800 ks. Similar to that of pearlite powders milled for 1800 ks, uniform equiaxed nanocrystalline ferrite with the grain size less than 10 nm was observed in the whole areas of powder (Fig. 7(a)). The SAD indicates that the cementite particles have dissolved completely. The HREM image (Fig. 7(b)) shows random orientation of the grains with large misorientation with neighbor grains. It should be noted that dislocations are not observed in the equiaxed nanocrystalline ferrite in both pearlite and spheroidite powders milled for

1800 ks.

The above SEM and TEM observations revealed that the microstructure evolution for nanocrystallization in ball milling is as follows. At the early stage of ball milling, the dislocation density increases and dislocation cell structure develops with milling time. With further ball milling, the misorientation between the adjacent cells increases and the size of dislocation cells decreases. When the dislocation density in the cell walls reaches a critical value, the transition from cellular to granular structure will take place to reduce the energy of the system as has been suggested.[5,6,14,18,27] It is considered that the severe and inhomogeneous deformation which occurs under high strain rate is an essential condition for this transition. The strain rate in ball milling is estimated to be 10^3–10^4 s^{-1}.[31] Under such a high strain rate, deformation occurs adiabatically. When a ball collides with a powder, the temperature of deformed region (surface of powder) increases and deformation will concentrate near the surface of powder. After a certain number of ball collisions, the surface area of powder reaches the critical dislocation density and transforms to nanocrystalline condition where the grain is either equiaxed 20 nm in diameter (in pearlite) or layered structure with 10–50 nm in thickness (in spheroidite). The boundary between the nanocrystalline ferrite and work-hardened regions are quite sharp as seen in Figs. 1(a) and (b). The formation mechanism of sharp boundary is considered as follows. Once the nanocrystalline region is produced near powder surface, the further ball collision will not deform the nanocrystalline region since the hardness is higher than 10 GPa. Instead the deformation will occur preferentially at work-hardened region adjacent to nanocrystalline region. This makes the sharp boundary between the nanocrystalline region and work-hardened regions. Ball milling produce a high strain rate deformation, which is very important for dislocations to reach the critical density to initiate the transformation from the cellular structure to granular one. This transformation can be considered as dynamic recovery and dynamic continuous recrystallization. Those phenomena are assisted by local temperature rise due to a large number of dislocation annihilation at cell walls.[27] From these consideration, it seems hard to produce nanocrystalline structure by conventional cold rolling because of low strain rate.

When the nanocrystalline ferrite grain is refined to around 10 nm, further refinement will not occur since deformation takes place mainly by grain boundary sliding.[32] Equiaxed nanocrystalline grains with random orientation and large misorientation will be achieved by grain boundary sliding (Fig. 7(b)).

3.1.2 Microhardness evolution

The microhardness evolution of pearlite and spheroidite powders with ball milling time is shown in Fig. 8. The starting microhardness of pearlite (3.3 GPa) is higher than that of spheroidite (2.2 GPa). The microhardness of the work-hardening regions in both pearlite and spheroidite powders increases with milling time up to 36 ks. The further milling up to 360 ks the change in the microhardness of work-hardening regions is small. The work hardened pearlite structure keeps higher microhardness than that of spheroidite structure. After 720 ks milling, the work-hardening region in the pearlite structure powder disappears, but it still remains in spheroidite structure powder. After milling for 1800 ks, the work-hardening region in spheroidite disappears.

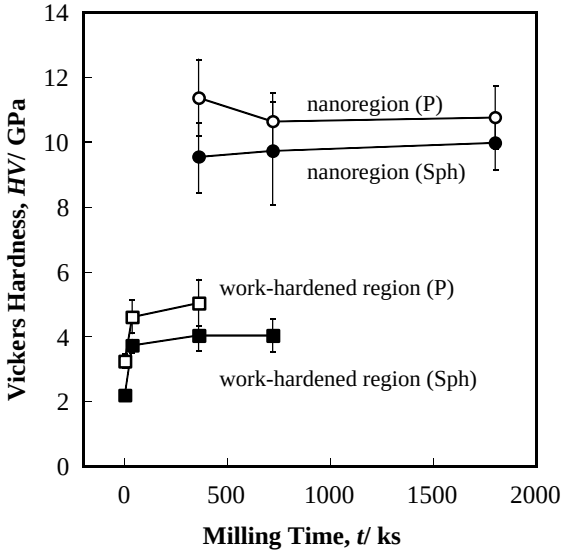

Fig. 8 Microhardness evolution of the work-hardening and nanocrystalline ferrite regions in the pearlite and spheroidite powders with milling time.

The microhardness of nanocrystalline ferrite region in pearlite powders milled for 360 ks is as high as 11.4 GPa, which is higher than that in the spheroidite powder milled for 360 ks (9.5 GPa). As mentioned above, the nanocrystalline ferrite in pearlite powder milled for 360 ks is equiaxed grain, while the nanocrystalline ferrite in spheroidite powder is mainly layered grain. This difference in grain size is considered to be responsible to the difference in the microhardness of nanocrystalline ferrite. Further milling up to 1800 ks does not make any significant change in the microhardness of nanocrystalline ferrite regions in both pearlite and spheroidite powders. It is considered that the measured microhardness of 1800 ks milled pearlite and spheroidite powders shown in the Fig. 8 is lower than the actual value, since the powder size is too small to be measured correctly after mounted in resin.

The distinct difference in microhardness between work-hardening region and nanocrystalline ferrite region indicates that the strengthening mechanisms of the two regions are different. It is considered that dislocation strengthening is responsible in the work-hardening region and grain refinement strengthening is responsible in the nanocrystalline ferrite region.[8]

3.2 Microstructure and microhardness evolution by annealing

3.2.1 Microstructure evolution by annealing

Figure 9 shows the annealed microstructures around the boundary between the work-hardening region (right hand side in each picture) and nanocrystalline ferrite region (left hand side in each picture) of the pearlite and spheroidite structure milled for 360 ks. After annealed at 673 K for 3.6 ks, only recovery takes place in the work-hardening regions of both pearlite and spheroidite structures (Figs. 9(a), (b)). The subgrains were observed by high magnification AFM in these regions. It is considered that in work-hardened pearlite fine cementite lamellae or fine cementite particles effectively pin the dislocations and grain boundaries and retard the recrys-

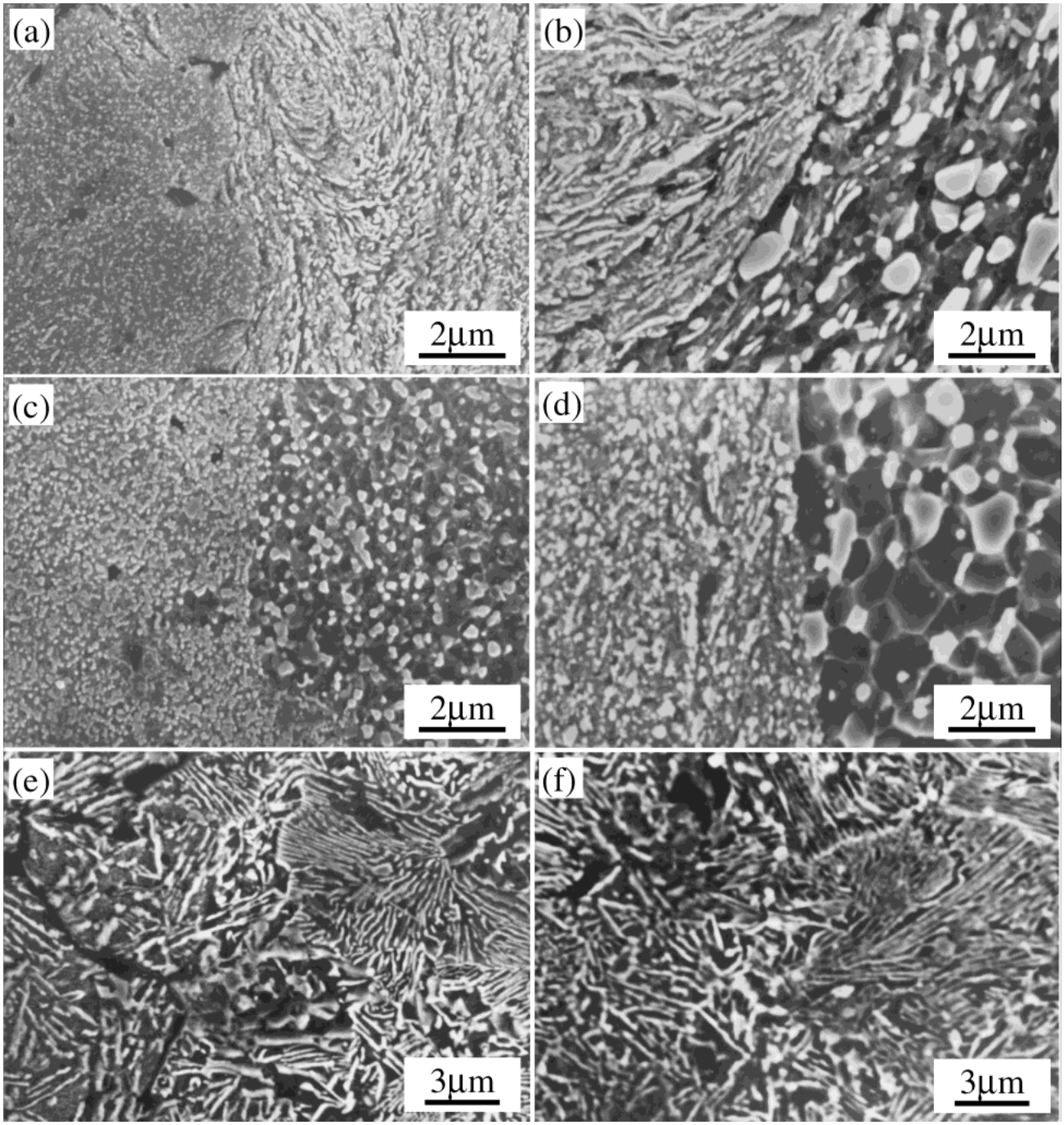

Fig. 9 Microstructure evolution of the work-hardening and nanocrystalline ferrite regions in the ((a), (c), (e)) pearlite and ((b), (d), (f)) spheroidite powders milled for 360 ks after annealing at (a), (b) 673 K; (c), (d) 873 K; and (e), (f) 1073 K for 3.6 ks respectively.

tallization of ferrite in the work-hardening regions. In the nanocrystalline ferrite regions of both pearlite and spheroidite structures (Figs. 9(a), (b)), the re-precipitation of fine cementite can be observed, but no significant change is seen in nanocrystalline ferrite grains. The size of re-precipitated cementite particle in pearlite powder is smaller than that in spheroidite powder.

When annealed at 873 K for 3.6 ks, recrystallization completes in the work-hardening ferrite region of pearlite structure leading to the formation of recrystallized ferrite grains with an average grain size of about 0.5 μm (Fig. 9(c)), while the grain growth of recrystallized ferrite to about 1.5 μm can be observed in the work-hardening ferrite region of spheroidite structure (Fig. 9(d)). In the nanocrystalline ferrite regions of pearlite and spheroidite structure (Figs. 9(c), (d)), the further re-precipitation and coarsening of cementite particles and the grain growth of nanocrystalline ferrite can be seen. It is considered that conventional discontinuous recrystallization does not take place in nanocrystalline ferrite region. The average grain size of nanocrystalline ferrite in the pearlite powder is smaller than that in spheroidite powder.

When annealed at 1073 K for 3.6 ks, the complete austenitization occurs, and pearlite structure formed during subsequent cooling (Figs. 9(e), (f)). The former nanocrystalline region and work-hardening region are still distinguishable since the former nanocrystalline ferrite region has less lamellar and

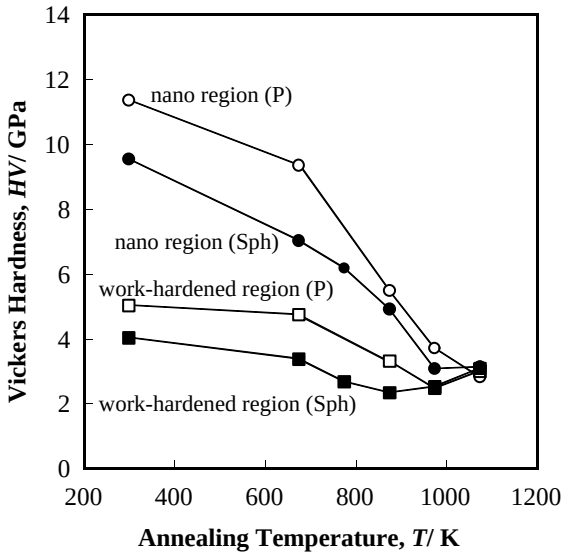

Fig. 10 Microhardness evolution of the work-hardening and nanocrystalline ferrite regions in the pearlite and spheroidite powders milled for 360 ks with annealing at different temperature for 3.6 ks.

more spherical cementite structure than that in the former work-hardening region. This difference in microstructure is due to the small γ grain size in the original nanocrystalline ferrite region. However, after annealed at 1273 K for 3.6 ks, the difference in pearlite microstructures between formed in the former nanocrystalline ferrite and work-hardening regions disappears, since the substantial grain growth of austenite occurs in both regions.

3.2.2 Microhardness evolution by annealing

Figure 10 shows the microhardness evolution of the work-hardened and nanocrystalline ferrite regions of pearlite and spheroidite powders as a function of isochronal annealing temperature. In both the work-hardened and nanocrystalline ferrite regions, the microhardness decreases with increasing annealing temperature up to 973 K. When the annealing temperature becomes higher than the eutectoid temperature, the microhardness of work-hardening regions increases since the microstructure changed from spheroidite to pearlite. With further increasing annealing temperature, the microhardness in work-hardening region decreases due to the recrystallization and grain growth. In contrast, the microhardness decrease in the nanocrystalline ferrite regions is attributed to the continuous grain growth of nanocrystalline ferrite and re-precipitation of cementite. The recrystallized ferrite grain size in work-hardening region formed from pearlite structure is smaller than that from spheroidite structure under the same annealing condition, hence the microhardness of recrystallization ferrite in pearlite powder is higher than that in spheroidite powder. Similarly, the grain size of annealed nanocrystalline ferrite formed from pearlite structure is finer than that from spheroidite structure under the same annealing condition, therefore the microhardness of annealed nanocrystalline ferrite in pearlite powder is higher than that in spheroidite powder.

4. Discussions

4.1 Comparison of nanocrystallization between pearlite and spheroidite

The microstructure in pearlite is much finer than that of spheroidite. When severe strain is applied to pearlite, the size of ferrite and cementite lamellae becomes smaller.[23,24] High density of dislocation cells forms in the ferrite lamellae of pearlite and divide the ferrite lamellae into subgrains. Equiaxed nanocrystalline ferrite will form when the dislocation cell structure transforms into granular structure by further deformation.[27] When severe strain is applied to the spheroidite structure, deformation of ferrite grain will first take place. The elongated subgrains will form inside the ferrite grains. Layered nanocrystalline ferrite will form when the dislocation cell structure transforms into granular structure. Layered nanocrystalline ferrite will evolve into equiaxed nanocrystalline ferrite with further deformation.

It is considered that the work-hardening rate of the material has an influence on the nanocrystallization rate. The pearlite structure characterized by higher work-hardening rate showed higher nanocrystallization rate than those of spheroidite. Pure iron has a lower work-hardening rate than that of high carbon steel. Ball milling of pure iron showed that layered nanocrystalline ferrite with an average thickness of around 100 nm and length of several hundreds nanometers forms after 360 ks of milling.[14] This indicates that the nanocrystallization rate of pure iron is slower than that of the Fe–0.89C steel with pearlite and spheroidite structures as is expected from the lower work-hardening rate.

4.2 Annealing behavior of nanocrystalline ferrite

The present results show that the annealing behavior of nanocrystalline ferrite is intrinsically different from that of work-hardening ferrite in both pearlite and spheroidite powders. Conventional discontinuous recrystallization takes place in the work-hardening ferrite region while a continuous grain growth takes place in the nanocrystalline ferrite region.

Grain growth occurs in polycrystalline materials to decrease the grain boundary energy. Nanocrystalline materials have a larger specific grain boundary area and the driving force for grain growth is higher than conventional materials. High grain growth rate is expected in the smaller grained materials. However, the low grain growth rate was observed in various nanocrystalline materials. The inherent stability of the nanocrystalline grains has been explained on the basis of structural factors such as narrow grain size distribution, equiaxed grain morphology, low energy grain boundary structures, relatively flat grain boundary configurations and porosity present in some samples.[33] Additionally, grain boundary Zener drag and triple junction drag have been found to be significant in retarding grain growth.[34] Zener drag (where a particle interacts with grain boundary to reduce the system energy and restrain the grain boundary movement) and solute drag can slow down the grain growth kinetics by reducing driving force or the grain boundary mobility. The carbon dissolved in the nanocrystalline ferrite is assumed to attribute to this effect. With the increase in annealing temperature, cementite particles begin to re-precipitate on the grain boundaries. The fine cementite particles prob-

ably work effectively to pin the movement of grain boundaries. Hence, the grain growth rate of nanocrystalline ferrite at lower annealing temperature is much lower than that of work-hardening ferrite. However, at higher annealing temperature (more than 873 K), the cementite particles become large due to the Ostward coalescence and the grain growth of nanocrystalline ferrite becomes large enough to be observed. It can be concluded that carbon and fine cementite particles in nanocrystalline ferrite have beneficial effect on the low grain growth rate of nanocrystalline ferrite in the ball milled pearlite and spheroidite powders.

It is also found that the grain growth rate of nanocrystalline ferrite formed from pearlite structure is slower than that from spheroidite structure. The grain size of nanocrystalline ferrite formed from pearlite structure is finer than that formed from spheroidite structure. Hence, the re-precipitated cementite is more finely and uniformly dispersed in the nanocrystalline ferrite region in pearlite structure than that in spheroidite structure powder. Consequently, larger effect on retarding the grain growth of nanocrystalline ferrite in pearlite than that of spheroidite structure powder.

5. Conclusions

The structural evolution by ball milling of an eutectoid steel with pearlite and spheroidite structures and their annealing behavior were compared in detail. SEM and TEM observations revealed that in both pearlite and spheroidite powders, the nanocrystallization starts from the surface of powders where the concentration of severe deformation is expected. The boundary between the nanocrystalline region and work-hardening region is sharp in both types of powders. The particle size reduction with milling time is faster, grain size in nanocrystalline ferrite at a given milling time is smaller and the dissolution of cementite is faster in pearlite than shperoidite. These results are considered to be due to higher work-hardening rate and smaller microstructure in pearlite than spheroidite. The annealing behaviors of nanocrystalline ferrite and work-hardening ferrite are intrinsically different. Conventional discontinuous recrystallization takes place in the work-hardening ferrite region, while continuous grain growth occurs in the nanocrystalline ferrite region during annealing. Under the same annealing condition nanocrystalline ferrite keeps higher microhardness than work-hardening ferrite. The thermal stability of nanocrystalline ferrite formed from pearlite structure is higher than that formed from spheroidite structure stemming from the finer original grain size.

Acknowledgments

This work is partly supported by the Grant-in-Aid for Scientific Research of the Japan Society for the Promotion of Science. The authors thank Dr. Z. G. Liu, Mr. Y. Aniya, Dr. X. J. Hao and Dr. Y. Todaka for their involvement. One of the authors (Y. Xu) would like to thank AIEJ for supplying scholarship to carry out this work in Japan.

REFERENCES

1) M. Jain and T. Christman: J. Mater. Res. **11** (1996) 2677–2680.
2) Y. Saito, N. Tsuji, H. Utsunomiya, T. Sakai and R. G. Hong: Scri. Mater. **39** (1998) 1221–1227.
3) R. Z. Valiev, A. V. Korznikov and R. R. Mulyukov: Phys. Met. Metall. **73** (1992) 373–383.
4) D. H. Shin, B. C. Kim, Y.-S. Kim and K.-T. Park: Acta Mater. **48** (2000) 2247–2255.
5) R. Z. Valiev, R. K. Islamgaliev and I. V. Alexandrov: Prog. Mater. Sci. **45** (2000) 103–189.
6) R. Z. Valiev, YU. V. Ivanisenko, E. F. Rauch and B. Baudelet: Acta Mater. **12** (1996) 4705–4712.
7) J. S. C. Jang and C. C. Koch: Scri. Mater. **24** (1990) 1599–1604.
8) S. Takaki and Y. Kimura: J. Jpn. Soc. Powder and Powder Metall. **46** (1999) 1235–1240.
9) C. C. Koch: Nanostruc. Mater. **2** (1993) 109–129.
10) H. J. Fecht, E. Hellstern, Z. Fu and W. L. Johnson: Metall. Trans. A **21A** (1990) 2333–2337.
11) C. C. Koch: Nanostruct. Mater. **9** (1997) 13–22.
12) H. J. Fecht: Nanostruct. Mater. **6** (1995) 33–41.
13) K. W. Liu, J. S. Zhang, J. G. Wang and G. L. Chen: J. Mater. Res. **13** (1998) 1198–1203.
14) J. Yin, M. Umemoto, Z. G. Liu and K. Tsuchiya: ISIJ Int. **41** (2001) 1389–1396.
15) H. H. Tian and M. Atsmon: Acta Mater. **47** (1999) 1255–1261.
16) Y. H. Zhao, H. W. Sheng and K. Lu: Acta Mater. **49** (2001) 365–375.
17) Z. G. Liu, X. J. Hao, K. Masuyama, K. Tsuchiya, M. Umemoto and S. M. Hao: Scri. Mater. **44** (2001) 1775–1779.
18) M. Umemoto, Z. G. Liu, X. J. Hao, K. Masuyama and K. Tsuchiya: Mater. Sci. Forum **360–362** (2001) 167–174.
19) M. Umemoto, Z. G. Liu, Y. Xu and K. Tsuchiya: Mater. Sci. Forum **386–388** (2002) 323–328.
20) K. Hono, M. Ohnuma, M. Murayama, S. Nishida, A. Yoshie and T. Takahashi: Scri. Mater. **44** (2001) 977–983.
21) H. G. Read, W. T. Reynolds Jr., K. Hono and T. Tarui: Scri. Mater. **37** (1997) 1221–1230.
22) M. H. Hong, W. T. Reynolds Jr., T. Tarui and K. Hono: Metall. Mater. Trans. A **30A** (1999) 717–727.
23) W. J. Nam, C. M. Bae, S. J. Oh and S. J. Kwon: Scri. Mater. **42** (2000) 457–463.
24) J. Languillaume, G. Kapelski and B. Baudelet: Acta Mater. **45** (1997) 1201–1212.
25) H. Hidaka, Y. Kimura and S. Takaki: J. Jpn. Soc. Powder and Powder Metall. **46** (1999) 1256–1260.
26) H. Hidaka, Y. Kimura and S. Takaki: Tetsu to Hagané **85** (1999) 52–58.
27) Y. Xu, Z. G. Liu, M. Umemoto and K. Tsuchiya: Metall. Mater. Trans. A, accepted.
28) C. H. Moelle and H. J. Fecht: Nanostruct. Mater. **6** (1995) 421–424.
29) T. R. Marlow and C. C. Koch: Acta Mater. **45** (1997) 2177–2186.
30) K. W. Liu and F. Mucklich: Acta Mater. **49** (2001) 395–403.
31) M. Umemoto, B. Hang, K. Tsuchiya and N. Suzuki: Scri. Mater. **46** (2002) 383–388
32) J. Karch, R. Birringer and H. Gleiter: Nature **330** (1987) 556–558.
33) C. Suryanarayana: Int. Mater. Rev. **40** (1995) 41–64.
34) K. Lu: Nanostruct. Mater. **2** (1993) 643–652.